Electronic Supplementary Information

for

Direct Surface Modification Strategy of ITO Anodes Enables High-Performance Organic Photodetectors

Jiahui Wang,[ab] *Ruyan Zhao,*[a] *Lu Zhang*,[a] *Junhui Miao*,*[a] *Jun Liu* *[ab] *and Lixiang Wang* [ab]

[a] State Key Laboratory of Polymer Physics and Chemistry, Changchun Institute of Applied Chemistry, Chinese Academy of Sciences, Changchun 130022, China.

[b] School of Applied Chemistry and Engineering, University of Science and Technology of China, Hefei 230026, China.

Contents

1. Measurements and Characterizations

UPS and XPS experiments were carried out in ultrahigh vacuum with a base pressure of 1×10^{-10} mbar utilizing an XPS/UPS system fitted with a VG Scienta R3000 analyzer. A monochromatized He Iα irradiation from discharged lamp supplies photons with 21.22 eV for UPS. A monochromatic Al (Kα) X-ray source provides photons with 1486.6 eV for XPS. The region of binding energy was swept between 190 eV and 215 eV 100 times for detecting the Cl 2p signal. UV-vis absorption spectra were measured with a PerkinElmer Lambda 35 UV-vis spectrometer. The surface morphologies of interlayer films were characterized using atomic force microscopy (AFM) on a SPA 300HV with a SPI 3800N controller (Seiko Instruments, Inc., Japan) in tapping mode. A silicon micro cantilever (spring constant 2 N m^{-1} and resonance frequency ca. 300 kHz, Olympus Co., Japan) with an etched conical tip was used for the scan. The contact angle was determined by the liquid drop shape analyzer (DSA10 from KRUSS Gmbh Germany). A XES-40S2-CE class solar simulator (Japan, SAN-EI Electric Co., Ltd.) was used to provide the AM 1.5G simulated solar light illumination. The light intensity was calibrated to be 100 mW cm^{-2} using a certified standard monocrystalline silicon (Si) solar cell (SRC-2020, Enli Technology Co., Ltd.). The *J–V* plots of the device were measured in a glove box filled with nitrogen (oxygen and water contents are smaller than 0.1 ppm) on a Keithley 2400 source meter. The responsivity was measured using a Solar Cell Spectral Response Measurement System QE-R3011 (Enlitech Co., Ltd.) under the short-circuit condition at a chopping frequency of 165 Hz. The electrical impedance spectroscopy tests were conducted using PARSTAT 3000A potentiostat at a frequency range from 10^5 Hz to 10 Hz without applied voltage. The noise current was measured by the ProPlus 9812D wafer-level 1/f noise characterization system. Film-depth dependent light absorption spectroscopy (FLAS) measurement was conducted by a Diener ZEPTO Plasma machine. The machine etched the blend film surface incrementally using low-pressure oxygen (0.1 MPa). With the etching time increasing, the thickness of blend films on different substrates gradually decreases. A PerkinElmer

Lambda 35 spectrometer recorded the UV–vis absorption spectra with each etching time of 100 seconds.

The hole mobilities were measured by the space-charge-limited current (SCLC) method. The hole-only device structure is Anode/active layer/MoO_3 (10 nm)/Al (100 nm). *J–V* plots in the range of 0–4 V were measured using a Keithley 2400 source meter, and the mobility was obtained by fitting the *J–V* plot near quadratic region according to the modified Mott-Gurney equation:

$$J = \frac{9}{8}\varepsilon_r\varepsilon_0\mu\frac{V^2}{L^3}\exp\left(0.89\beta\frac{\sqrt{V}}{\sqrt{L}}\right) \#(1)$$

Where J is the current density, ε_0 is permittivity of free space, ε_r is the relative permittivity (assumed to be 3), μ is the zero-field mobility, V is the potential across the device ($V = V_{applied} - V_{bi} - V_{series}$), L is the thickness of active layer, and β is the field-activation factor. The hole mobilities were averaged from 6 devices.

2. XPS spectra

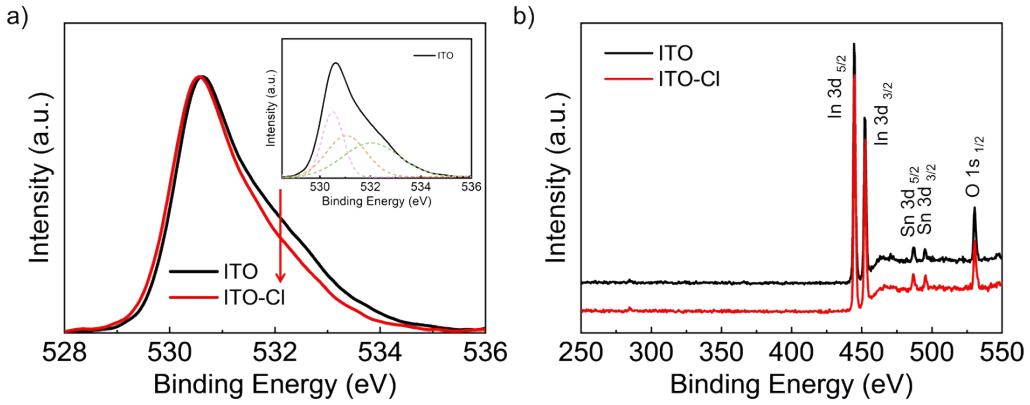

Figure S1. a) XPS spectra of O 1s for ITO and ITO-Cl anodes. The inset is the fitting XPS spectra of ITO. b) Offset XPS spectra for ITO and ITO-Cl anodes.

The O 1s peak can be fitted with three components, where the peak at 532.05 eV corresponds to In^{3+}–OH^- bond. The peak intensity of In^{3+}–OH^- bond is decreased in ITO-Cl surface in comparison with the ITO. That suggested that the hydroxyl groups on the ITO surface were replaced by chlorine atoms after HCl aqueous solution soaking. The Sn:In ratios are 0.254 for bare ITO and 0.176 for ITO-Cl. The decreased Sn:In ratio

in ITO-Cl suggests that the coverage of Sn on the ITO surface reduced after HCl soaking.

3. Transmission spectra

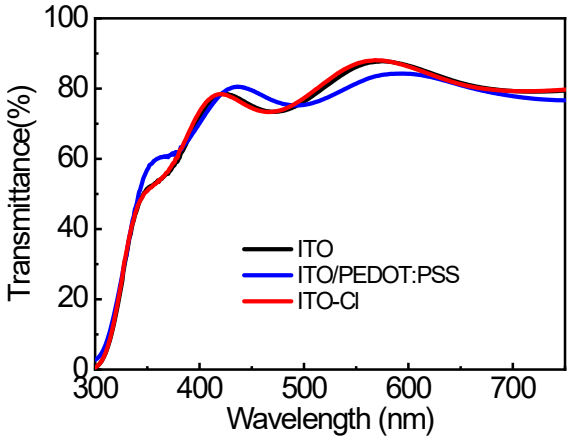

Figure S2. Transmission spectra of different anodes.

4. Absorption spectra

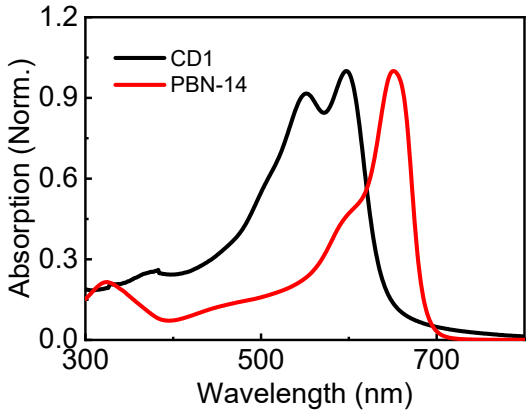

Figure S3. Absorption spectra of CD1 and PBN-14 in thin film.

5. OPD performance

5.1 HCl concentration optimization

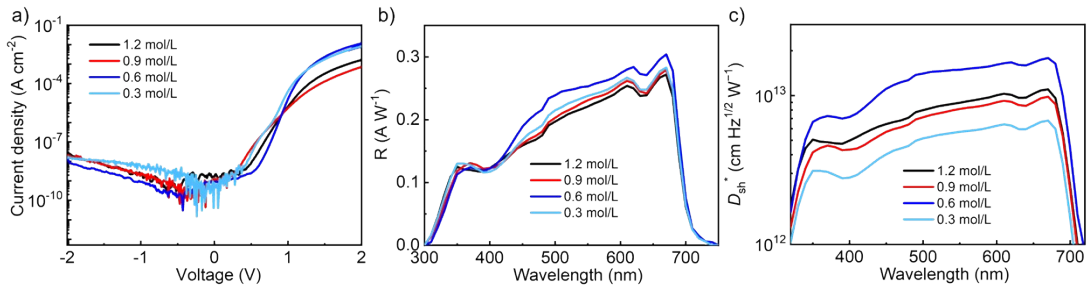

Figure S4. a) $J-V$ curves in dark. b) Responsivity at −1 V. c) D_{sh}^{*} spectra of the OPD devices with various HCl concentration under −1 V applied voltage.

We compared the device performance using HCl-soaked ITO anodes with various HCl concentration (0.3, 0.6, 0.9 and 1.2 mol/L). For various HCl concentrations, all the ITO-Cl-based devices exhibit one order of magnitude lower dark current density (J_d) than ITO/PEDOT:PSS-based devices. Among them, the concentration of 0.6 mol/L shows the highest responsivity (R). When the HCl concentration is 0.3 mol/L, the less distribution of Cl atoms on the ITO surface may affect the work function of the anode, which is unfavorable for electron blocking. This is consistent with the high dark current of the device. Soaking ITO with a high concentration of HCl (>0.6 mol/L) may roughen their surfaces, and affect the extraction of holes, which is related to the low responsivity of the device. The optimized HCl concentration for the ITO surface modification is 0.6 mol/L.

5.2 OPD performance at 0 V

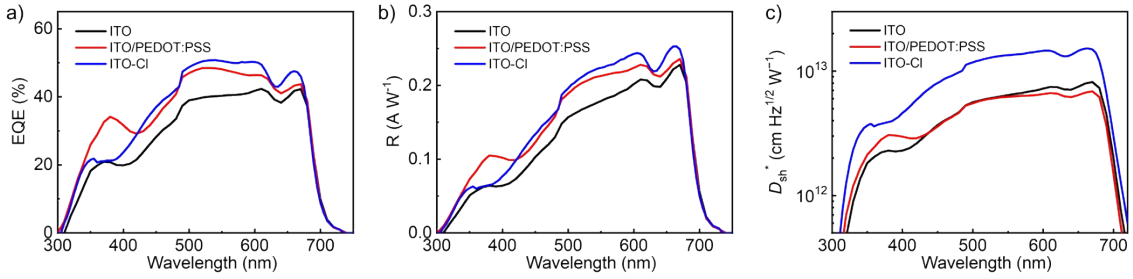

Figure S5. a) EQE curves. b) Responsivity. c) D_{sh}^* spectra of the OPD devices with different anodes under 0 V applied voltage.

We measured the EQE curves and responsivity of OPD devices with different anodes under zero bias. The higher EQE and R values imply that the ITO-Cl anode improved charge generation and transport. Under 0 V bias, the ITO-Cl-based device presented a prominent maximum D_{sh}^* of 1.51 × 10^{13} cm $Hz^{1/2}$ W^{-1}.

5.3 Average value and standard deviation data of the OPD devices at −1 V bias.

Table S1. Performance of the OPD devices with different anodes.

Anodes	$J_{d,-1V}$ (A cm^{-2})	$D_{sh}^{*}{}_{-1V}$ [a)] (cm $Hz^{1/2}$ W^{-1})
ITO	(5.95 ± 0.9) × 10^{-7}	(6.63 ± 0.3) × 10^{11}
ITO/PEDOT:PSS	(5.99 ± 0.4) × 10^{-8}	(2.17 ± 0.2) × 10^{12}
ITO-Cl	(9.03 ±0.4) × 10^{-10}	(1.79 ± 0.2) × 10^{13}

[a)] Average value and standard deviation data are calculated from 6 devices.

6. AFM images

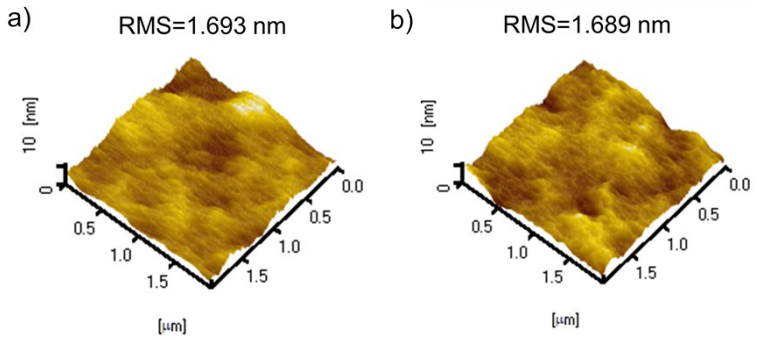

Figure S6. 3D AFM topography images of CD1:PBN-14 blend films on the top of a) ITO/PEDOT:PSS and b) ITO-Cl. The AFM imaging size is 2 µm × 2 µm.

7. Surface energy

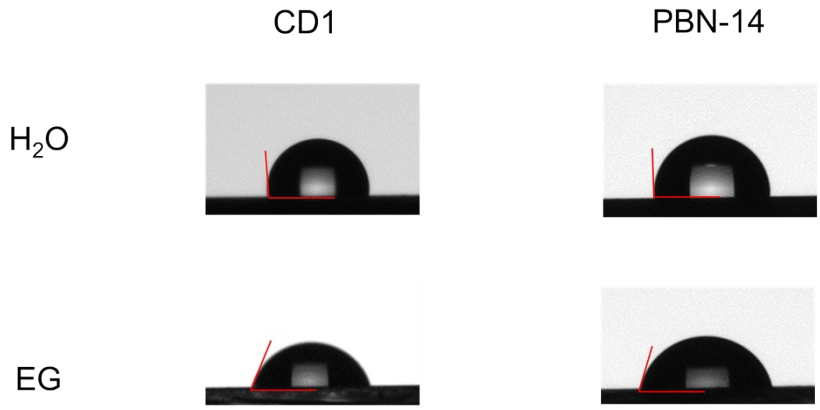

Figure S7. Contact angle of water and ethylene on CD1 and PBN-14 films.

Table S2. The contact angles and surface energy parameters of the CD1 and PBN-14 films.

	θ_{H_2O}	θ_{EG}	γ_d (mJ m^{-2})	γ_p (mJ m^{-2})	γ (mJ m^{-2})
CD1	94.2°	69.2°	23.14	2.41	25.55
PBN-14	94.5°	73.1°	17.63	3.81	21.44